Nitrogen vacancy center in cubic silicon carbide: A promising qubit in the 1.5 μm spectral range for photonic quantum networks

S. A. Zargaleh,[1,*] S. Hameau,[2] B. Eble,[2] F. Margaillan,[2] H. J. von Bardeleben,[2,†] J. L. Cantin,[2] and Weibo Gao[1,3]

[1]*Division of Physics and Applied Physics, School of Physical and Mathematical Sciences, Nanyang Technological University, Singapore 637371, Singapore*

[2]*Sorbonne Université, Campus Pierre et Marie Curie, Institut des NanoSciences de Paris, 4, place Jussieu, 75005 Paris, France*

[3]*The Photonics Institute and Centre for Disruptive Photonic Technologies, Nanyang Technological University, Singapore 637371, Singapore*

(Received 21 July 2018; published 15 October 2018)

We have investigated the optical properties of the nitrogen vacancy $(NV)^-$ center in 3C-SiC to determine the photoluminscence zero phonon line (ZPL) associated with the $^3E \rightarrow {}^3A_2$ intracenter transition. Combining electron paramagnetic resonance and photoluminescence spectroscopy, we show that the NV^- center in 3C-SiC has a ZPL line at 1.468 μm in excellent agreement with theoretical predictions. The ZPL line can be observed up to $T = 100$ K. The negatively charged NV center in 3C-SiC is the structural isomorphe of the NV center in diamond and has equally a spin $S = 1$ ground state and a spin $S = 1$ excited state, long spin lattice relaxation times and presents optically induced groudstate spin polarization. These properties make it already a strong competitor to the NV center in diamond, but as its optical domain is shifted in the near infrared at 1.5 μm, the NV center in 3C-SiC is compatible with quantum photonic networks and silicon based microelectronics.

DOI: 10.1103/PhysRevB.98.165203

I. INTRODUCTION

The coherent manipulation, measurement, and entanglement of individual solid-state spins using optical excitation has recently become a field of high interest in light of their future applications for photonic quantum computing, network, and communication. In recent years, one solid-state based system has turned out to be particular promising in this field: the NV center in diamond, i.e., a carbon vacancy nitrogen donor close-pair defect. For a recent review see Doherty et al [1]. The question whether the NV center in diamond is unique or whether similar defects could be generated in other materials has been the object of theoretical studies [2–8]. These studies suggested that it would be highly desirable to engineer defects with comparable spin and optical properties in more technological materials such as SiC, which would also allow scalability. Two Si vacancy-related defects in SiC (V_{Si}, $V_{Si}V_C$) have already confirmed the exceptional magneto-optical properties predicted [9]. We have recently identified by electron paramagnetic resonance (EPR) spectroscopy and first-principle calculations of its spin Hamiltonian parameters the negatively charged NV centers in SiC. In SiC, NV centers are ($V_{Si}N_C$) nearest neighbor pairs. We have generated them in the three polytypes 3C, 4H, 6H of SiC [10–14] and have determined their ground-state spin properties by EPR. They have the same electronic structure with a $^3A_2$ ground state, a ^3E excited state, and an associated intracenter radiative transition in all three polytypes. Among the SiC polytypes, 3C-SiC is a special case, as it has the higher symmetry zinc-blende crystal structure and contains only one type of NV center with C_{3V} symmetry. Concerning the magneto-optical properties, they have been obtained for the NV centers in 4H-SiC but not yet for those in 3C-SiC. In particular, the zero phonon emission line (ZPL) of the NV^- center has not yet been reported. In diamond, the NV^- center has a ZPL in the visible (637 nm), a spectral range which is not well suited for quantum technology (QT) applications. It would be desirable to shift this spectral range further into the telecommunication C-band range around 1.5 μm and indeed, such a spectral range has been predicted for the NV^- center ZPL in 3C-SiC. The motivations to study NV centers in 3C-SiC as well as in the other SiC polytypes are numerous as they open new perspectives for QT-related applications and nanosensing. They are associated with the superior material properties and the different defect properties: SiC is a high-tech material applied already in numerous microelectronics devices and as compared to diamond of low cost. Further, 3C-SiC can be epitaxially grown on silicon substrates, which makes its integration in standard microelectronic technology feasible. Concerning the defect properties: a first and major difference is that the optical range of the ZPL PL lines are shifted from the visible to the near infrared. Further, its smaller band gap shifts the $2-/1-$ charge transition level in the conduction band and thus stabilizes the NV center fully in the $1-$ charge state in n-type material. In this paper, we present the results of a combined photo EPR and photoluminescence (PL) spectroscopy study from which we evidence and assign the ZPL PL line of the NV^- center.

*Previous address: Sorbonne Université, Campus Pierre et Marie Curie, Institut des NanoSciences de Paris, 4, place Jussieu, 75005 Paris, France; az.soroush@gmail.com; soroush.abbasi@insp.jussieu.fr

†vonbarde@insp.jussieu.fr

II. EXPERIMENTAL

The 3C-SiC samples were freestanding, *n*-type nitrogen doped, (100) oriented layers of 300 μm thickness; the Nitrogen doping level was 2×10^{16} cm^{-3}. For the EPR and PL measurements, the samples were cut to 3×6 mm^2 with the long axis parallel to [110]. The NV centers were generated in a two-step process, consisting of (i) the formation of Si vacancies by proton irradiation, followed by (ii) a thermal annealing at temperatures, where the V_{Si} become mobile and form close pairs with the N_C dopant. In this annealing step, divacancy centers ($V_{Si}V_C$) are equally generated in parallel as the formation of carbon vacancies cannot be avoided in step (i). Here we used high energy proton (6 MeV) irradiation at fluences of $10^{15} - 10^{16}$ cm^{-2} for the V_{Si} generation; the samples were then annealed at 800 °C. To monitor the formation of NV centers, we performed *X*-band EPR measurements with a commercial EPR spectrometer (Bruker) in the 4 K to 300 K temperature range. We investigated equally the photo EPR properties of the NV center as the spectral dependence of the excitation process provides information about the energy of the first excited state. We scanned in particular the 1000 nm to 1400 nm range, which is relevant for this center. For this we used a quartz halogen lamp as a white light source and a Czerny-Turner monochromator for the wavelength selection. The excitation power in this case is low (<0.1 mW e) but this turned out to be sufficient to induce the spin polarization. The spectral resolution for the measurement is 15 nm.

The PL measurements were performed on the same samples characterized by EPR. The samples were excited with a ps Ti sapphire laser, which pumped an optical parametric oscillator (OPO); this allowed us to scan different excitation wavelengths. The PL measurement was performed with an excitation normal to the film plane and perpendicular to the plane. The excitation was focused onto the sample with a 0.5 NA microscope objective and the PL was dispersed by a 0.5 m focal length spectrometer providing a 40 μeV spectral resolution. The PL was detected with a cooled InGaAs detector. The PL measurements were mainly performed at $T = 20$ K. We measured in addition the temperature dependence of the PL spectra up to $T = 100$ K.

III. RESULTS

A. EPR and photo-EPR spectroscopy

In Fig. 1, we show a typical low temperature EPR spectrum of an irradiated and annealed sample under photoexcitation. The orientation of the applied magnetic field is parallel to the [111] axis. The spectrum is characterized by the presence of three spin $S = 1$ centers with C_{3V} symmetry. Two of them have been reported before and attributed based on their spin Hamiltonian parameters (Table I) to the neutral divacancy $(V_{Si}V_C)^0$ and the negatively charged NV$^-$ center, respectively. The third spectrum, labeled X here, had not been reported before. As it does not show resolved hyperfine interaction, it will not be further discussed here. The C_{3V} symmetry of the centers had been deduced from the angular variation of the resonance fields for a rotation in the (110) plane (not shown here). Due to the random generation of the defects by the irradiation/annealing procedure, centers aligned

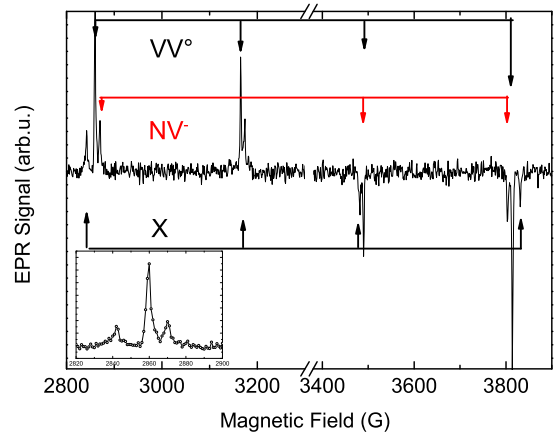

FIG. 1. Large-scale EPR spectrum of an irradiated and annealed 3C-SiC sample for B ∥ [111]. The spectrum shows three sets of [111] oriented spin $S = 1$ centers, which are labeled VV^0, NV$^-$, and X. The insert shows the low part of the spectrum at higher resolution.

along any of the four [111] directions will be formed with equal probabilities. We observe thus for an orientation of the magnetic field B ∥ [111] for each of the three centers: one two-line EPR spectrum corresponding to the parallel oriented and one two-line spectrum for the three 109° orientated centers, which are degenerate for this orientation. The EPR parameters of the NV$^-$ and VV^0 centers given in Table I are also compared to those of the NV center in diamond. The parameters are defined by the spin Hamiltonian for a spin $S = 1$ center with conventional notation:

$$H = S \cdot g \cdot B + S \cdot D \cdot S + S \cdot A_k \cdot I_k. \quad (1)$$

An important fingerprint of the NV$^-$ center, which distinguishes it from the VV^0 center, is the hyperfine interaction (HF) between the electron spin $S = 1$ and the $I = 1$ ^{14}N nuclear spin, already partially resolved in the EPR spectrum (Fig. 2). This results in a characteristic "triplet" structure. We show also in Table I the known ZPL PL parameters for the VV^0 center in 3C-SiC and the NV$^-$ center in diamond as well as the predicted values for the NV$^-$ center in 3C-SiC.

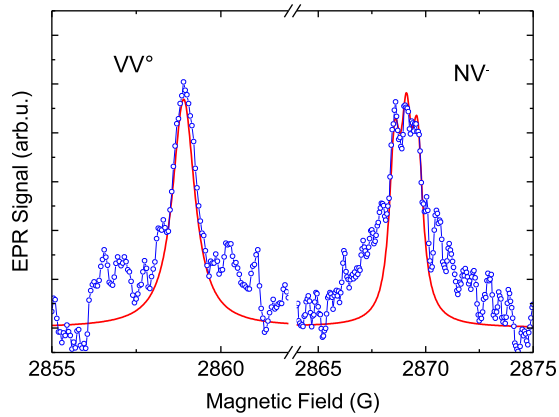

FIG. 2. High-resolution EPR spectrum of the low field VV^0 and NV$^-$ related EPR lines observed under photo excitation; the triplet structure of the NV center spectra reveal the HF interaction with the nuclear spin $I = 1$ of ^{14}N; T = 4 K, B ∥ [111].

TABLE I. Spin Hamiltonian parameters of the NV^- and VV^0 centers in 3C-SiC and the NV^- center in diamond; we show the Landé g-factors g, the zero-field splitting parameter D, the superhyperfine interaction parameters A, and the wavelength of the NV^- center ZPL photoluminescence line.

Center	$g_\perp$ [111]	$g_\parallel$ [111]	D^{exp} (MHz)	$A^{exp\ 14}N$ (MHz)	$A^{DFT\ 14}N$ (MHz)	$A^{DFT}6\times$ Si (MHz)	$A^{DFT}3\times$ Si Si (MHz)	$A^{DFT}3\times$ C (MHZ)	ZPL^{DFT} (nm)	ZPL^{exp} (nm)
NV^- 3C	2.003	2.004	1303	1.26	−1.08	8.00	10.3	135/64	1393 [8] 1425 [13] 1442 [12]	1468
VV^0 in 3C	2.003	2.003	1336	–	–	–	10	136/67 122/52		1105 [15,16]
NV^- Diamond	2.0028	2.0028	2880	2.3	2.3/2.7	–	–	201/120	634	637

From the EPR characterization, we can conclude that we have successfully generated NV^- and VV^0 centers by this approach and that they are the dominant species in these samples.

We then performed photo EPR measurements with *in situ* excitation to obtain further information on the NV center. The NV center in 3C-SiC has an electronic structure similar to the NV center in diamond with a $^3A_2$ ground state, a ^3E excited state and an intermediate ^1A singlet state. This particular electronic structure is common to all NV^- centers in SiC and diamond. The presence of an ^1A singlet state leads to on optically induced ground-state spin polarization when the NV^- center is excited into the ^3E state. The ground state becomes spin polarized in the $m_s = 0$ state due to a recombination via the ^1A singlet state, which operates in parallel to the radiative transition $^3E \rightarrow {}^3A_2$. The optically induced ground-state spin polarization of the NV^- center is observed in EPR by a strong increase of the EPR signal intensity and a phase inversion for the high field and low field lines. Monitoring the EPR signal intensity allows thus a measurement of the optical absorption process $^3A_2 \rightarrow {}^3E$. We have measured the photo excitation in the range 1000 nm to 1400 nm with a broadband white light source coupled to a monochromator system. (Fig. 3). The excitation power of this system is of the order of 100 nW, sufficient to observe the GS polarization. For longer wavelengths, the photon flux is to low. The results are given in Fig. 3. They contain two important pieces pf information: first, the NV^- center can be excited in the ^3E state even at wavelengths above 1300 nm. This indicates that the ZPL PL line must be situated at still longer wavelengths. Second, we observe a peak in the absorption spectrum at 1280 nm, which in a first approach we assign to a phonon-assisted transition of the $^3A \rightarrow {}^3E$ absorption. Indeed, this wavelength corresponds to a shift of about 120 meV from the ZPL line at 1468 nm, which we will attribute in the following to the NV^- center. It is in good agreement with the longitudinal optical (LO) phonon energies of 3C-SiC.

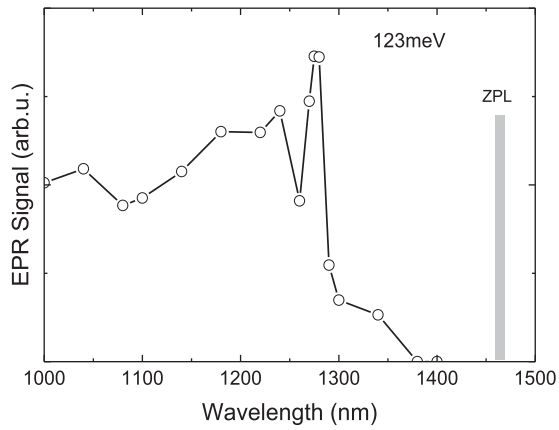

FIG. 3. Optical excitation spectrum of the NV^- center as measured by photo EPR with a broadband white light/monochromator system. It displays one broad excitation band with a narrow line at 1280 nm. Beyond 1400 nm, the available photon flux is to low to allow photo excitation. We indicate also by a bar the ZPL of the NV^- assigned from our results. The line at 1280 nm is at 123 meV from the ZPL.

B. PL spectroscopy

The samples thus prepared were investigated by PL under different below-band-gap excitation conditions. A picosecond mode-locked Ti:sapphire laser at a fixed wavelength is used to pump an OPO, generating the signal and idler output train of pulses, which allowed us to vary the excitation wavelength between 900 nm and 1300 nm. When excited at 940 nm (Fig. 4), the PL spectrum is dominated by one narrow ZPL at 1105 nm, which can be associated with the VV^0 center. The

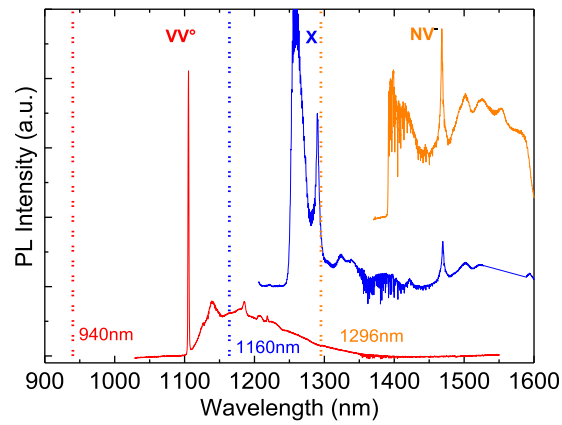

FIG. 4. Large-scale PL spectra as measured for different excitation wavelengths indicated by dotted vertical lines. We observe three distinct ZPL emission lines at 1105 nm (VV^0), 1290 nm (X Center), 1468 nm (NV^-). The broad line at 1270 nm is a system-related artifact. The spectrum between 1350 nm and 1400 nm is due to water absorption.

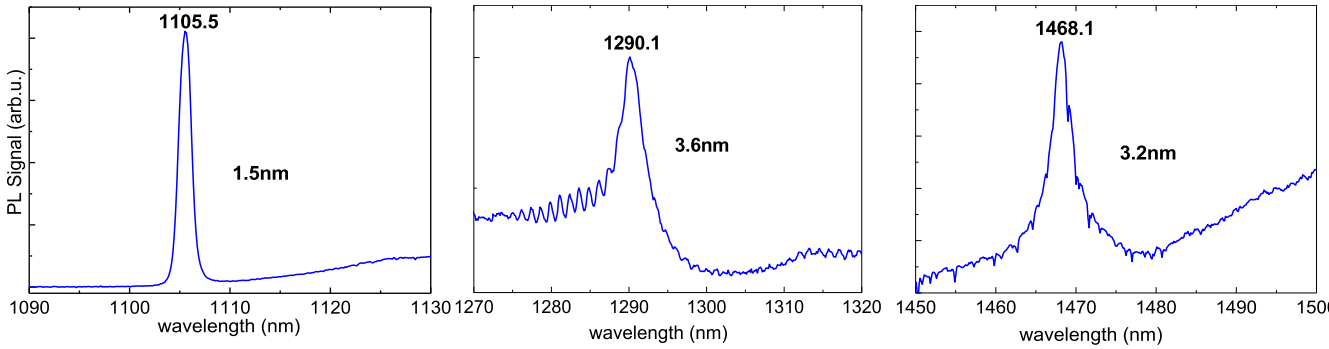

FIG. 5. High-resolution spectra of the three ZPL lines.

identification of the microscopic structure of the $(V_{Si}V_C)^0$ center and the association with the 1108 nm ZPL, corresponding to the $^3E \rightarrow {}^3A_2$ transition, has only been achieved recently by optically detected magnetic resonance spectroscopy via the specific zero-field splitting parameter D and the resolved hyperfine (HF) structure with ^{13}C and ^{29}Si neighbors [15,16]. When excited at a longer wavelength of 1160 nm, we observe two ZPL lines at 1290 nm and 1468 nm. The broad line 1270 nm is a system artefact. When excited at a still higher wavelength (1296 nm), we observe the ZPL at 1468 nm with increased intensity. The linewidth of this ZPL is 3.2 nm. This wavelength is close to the one predicted by *ab initio* calculations of 1442 nm (see Fig. 5). All three ZPL lines are accompanied by side bands originating from acoustic phonon emission. These broad bands lead to unwanted fringes of constructive and destructive interference localised on the CCD plane, which artificially modulate and/or pattern the spectrum. In Fig. 5, we show the three ZPL at higher resolution.

To further investigate the properties of the 1468 nm ZPL, we have performed polarization-resolved PL measurement from which we can deduce the symmetry of the related center. It consists of recording the luminescence intensity for a fixed orientation of the detection polarizer (placed in front of the spectrometer slit) as a function on the excitation polarization direction (controlled with a lambda/2 wave plate). Thus, the contrast defined by C = (Imax-Imin)/(Imax+Imin) can be extracted to construct the polarization indicatrix (PI) in polar coordinates. The shape of the PI is able to probe the local symmetry of the point defect. Thus for the zinc-blende crystal symmetry, the polarization indicatrix of a center with C_{3V} symmetry should be the result of the interference pattern between four degenerate emitting electric dipoles oriented along the [111], [1-1-1], [-11-1], and [-1-11] directions. We have analyzed the PL polarization for the excitation normal to the (001) crystal surface. In this configuration, the polarization indicatrix associated to (2+2) equivalent defects should present a rotational symmetry of order 4. A similar approach was used in Ref. [17] for the case of diamond where the PI relative to NV^0 or NV^- present four distinct lobes. Our results are presented in Fig. 6.

We observe as expected for such symmetry four lobes, pointing in the direction defined by the projection of the point defect orientations in the (100) plane. This confirms the C_{3V} symmetry of the centers giving rise to the 1468 nm ZPL. A particular feature is the fact that the polarization C for $\phi = 45^\circ$ mod 90° is clearly different from 0. We attribute this to an interference effect between the four optical dipoles; this is consistent with the optical response from degenerate wavelength emissions, as expected for the NV centers in 3C-SiC. The PI can be fitted by introducing a mutual coherence between the dipolar electric fields. This simple approach gives a good fit to the experimental data. The contrast for $\phi = 45^\circ$ mod 90° slightly decreases when increasing the laser excitation energy (not shown) [17], suggesting that the polarization-selective dipole excitation becomes less efficient.

A priori, we have thus two candidates for the ZPL of the NV^- center: the ZPL at 1290 nm and the ZPL at 1468 nm. However, the information obtained from the photo-EPR results allows to exclude the 1290 nm ZPL line. As the photo EPR results have shown that the ground-state spin polarization of the NV center can be induced by excitation with a wavelength above 1290 nm, the ZPL of the NV^- center must be at a longer wavelength which indicates the 1468 nm ZPL. The polarization measurements have also confirmed the C_{3V} symmetry of the centers related to the 1468 nm ZPL line, the known point symmetry of the NV^- center. Our EPR and PL results thus give strong evidence to assign the 1468 nm ZPl to the NV^- in 3C-SiC. This assignment is consolidated by

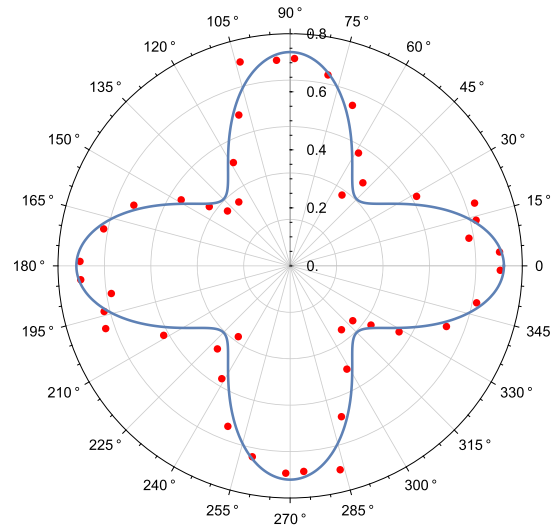

FIG. 6. Polarization indicatrix of the ZPL at 1468 nm, which we attribute to the NV^- center internal transition.

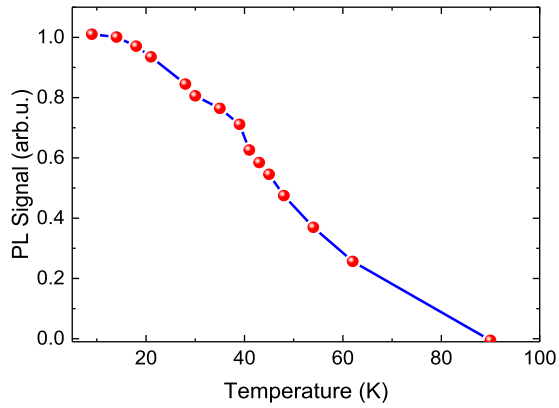

FIG. 7. Temperature dependence of the 1468 nm ZPL PL line.

three different first-principle calculations, which predict the NV^- ZPL line to be in the range of 1400 nm: Ref. [8] predicts a wavelength of 1393 nm (0.89 eV), Ref. [12] a wavelength of 1442 nm (0.86 eV), Ref. [13] a wavelength of 1425 nm (0.87 eV). Given the precision with which these energies can be calculated, the agreement between these predictions and the experimental value of 1468 nm (0.845 eV) can be considered as satisfactory.

Finally, we have investigated the temperature dependence of the 1468 nm ZPL (Fig. 7). For applications in QT and nanosensing, the temperature range in which the ZPL can be observed is of great importance. We observe the ZPL upto a temperature of $T = 100$ K with a linear decrease for temperatures above $T = 20$ K.

IV. CONCLUSION

In conclusion, by combining EPR, photo EPR, PL, and polarization spectroscopy, we have been able to assign the 1468 nm ZPL emission to the internal transition $^3E \rightarrow {}^3A_2$ of the NV^- center. This assignment, which is in excellent agreement with theoretical predictions, demonstrates the particular optical properties of the NV^- center in 3C-SiC, which will make it the most suited one for QT application. Whereas the NV^- centers in the two other main polytypes 4H and 6H have ZPL emitting in the 1200-nm range, the different structures of the cubic polytypes shifts this spectral range in the telecommunication band. In addition, and contrary to the 4H and 6H polytypes, the 3C polytype can be easily epitaxied on silicon substrates, which make it the favorite candidate for integration in standard microelectronic devices.

ACKNOWLEDGMENTS

S.A.Z. wishes to acknowledge the generous support from the international Merlion Grant France-Singapour and the Quantum Nanophotonic Laboratories at NTU Division of Physics and Applied Physics, School of Physical and Mathematical Sciences. The authors acknowledge financial support from the Merlion Program France Singapore No. 2.06.16. We thank Uwe Gerstmann (University of Paderborn, Germany) for the communication of the hyperfine interactions and fruitful discussions on theoretical predictions of ZPL energies.

[1] M. W. Doherty, N. B. Manson, P. Delaney, F. Jelezko, J. Wrachtrup, and L. C. L. Hollenberg, Phys. Rep. **528**, 1 (2013).
[2] F. Pan, M. Zhao, and L. Mei, J. Appl. Phys. **108**, 043917 (2010).
[3] J. R. Weber, W. F. Koehl, J. B. Varley, A. Janotti, B. B. Buckley, C. G. Van de Walle, and D. D. Awschalom, Proc. Natl. Acad. Sci. **107**, 8513 (2010).
[4] D. DiVincenzo, Nat. Mater. **9**, 468 (2010).
[5] J. R. Weber, W. F. Koehl, J. B. Varley, A. Janotti, B. B. Buckley, C. G. Van de Walle, and D. D. Awschalom, J. Appl. Phys. **109**, 102417 (2011).
[6] A. Dzurak, Nature **479**, 47 (2011).
[7] A. Boretti, Nat. Photonics **8**, 88 (2014).
[8] L. Gordon, A. Janotti, and C. G. Van de Walle, Phys. Rev. B **92**, 045208 (2015).
[9] P. G. Baranov, A. P. Bundakova, A. A. Soltamova, S. B. Orlinskii,I. V. Borovykh, R. Zondervan, R. Verberk, and J. Schmidt, Phys. Rev. B **83**, 125203 (2011).
[10] H. J. Von Bardeleben, J. L. Cantin, E. Rauls, and U. Gerstmann, Phys. Rev. B **92**, 064104 (2015).
[11] S. A. Zargaleh, B. Eble, S. Hameau, J. L. Cantin, L. Legrand, M. Bernard, F. Margaillan, J. S. Lauret, J. F. Roch, H. J. Von Bardeleben, E. Rauls, U. Gerstmann, and F. Treussart, Phys. Rev. B **94**, 060102 (2016).
[12] H. J. Von Bardeleben, J. L. Cantin, A. Csóré, A. Gali, E. Rauls, and U. Gerstmann, Phys. Rev. B **94**, 121202 (2016).
[13] A. Csóré, H. J. Von Bardeleben, J. L. Cantin, and A. Gali, Phys. Rev. B **96**, 085204 (2017).
[14] H. J. Von Bardeleben and J. L. Cantin, MRS Communications **7**, 591 (2017).
[15] S. A. Zargaleh, Spectroscopie d'excitation de la photoluminescence à basse température et resonance magnétique détectée optiquement de défauts paramagnétiques de spin S = 1 carbure de silicium ayant une photoluminescence dans le proche infrarouge, Ph.D. thesis, Paris Saclay 2017.
[16] D. J. Christle, P. V. Klimov, C. F. d. l. Casas, K. Szász, V. Ivády, V. Jokubavicius, J. U. Hassan, M. Syväjärvi, W. F. Koehl, T. Ohshima, N. T. Son, E. Janzén, A. Gali, and D. D. Awschalom, Phys. Rev. X **7**, 021046 (2017).
[17] D. Braukmann, V. P. Popov, E. R. Glaser, T. A. Kennedy, M. Bayer, and J. Debus, Phys. Rev. B **97**, 125426 (2018).